

Thermodynamics of Carbon in Nickel, Iron-Nickel and Iron-Chromium-Nickel Alloys

K. NATESAN AND T. F. KASSNER

Iron-nickel alloys with 8 and 16 wt pct nickel and iron-chromium-nickel alloys with 8 pct nickel and chromium contents in the range of 2 to 22 pct were equilibrated with iron and nickel in flowing CH₄-H₂ gas mixtures and in sealed capsules under partial vacuum at temperatures between 700 and 1060°C. Carbon activities in these alloys were established from the carbon concentrations in the nickel by applying Henry's law to the solubility of carbon in nickel that was determined in the temperature range of 500 to 1000°C. First-order free-energy interaction parameters were used to relate the carbon activities to composition and temperature in the single-phase austenitic Fe-Ni and Fe-Cr-Ni alloys. An expression was also developed to evaluate carbon activities in Fe-Cr-Ni alloys in the region of higher chromium contents (>4 wt pct) that result in a two-phase austenite plus carbide mixture at these temperatures.

IRON-base alloys with variations in the chromium and nickel concentrations form the basis of a number of austenitic stainless steels that have extensive high-temperature application in turbines, steam generators, and piping in electric power generating plants; in gas cracking and reforming facilities in the petroleum refining industry; and in sodium-cooled fast-breeder nuclear reactors for the fuel cladding, heat exchangers, piping, valves, and various structural components. Although the environmental conditions are vastly different in these applications, the materials in general change in microstructure and composition, primarily in the nonmetallic elements such as carbon, nitrogen, and boron, after long-term service at high temperatures. The relationship between the composition, microstructure and mechanical properties of these materials has been the subject of numerous investigations.¹⁻¹⁰ The importance of the carbon and nitrogen contents in these steels on the microstructural stability¹¹⁻¹⁴ and the mechanical behavior⁵⁻⁹ is also well recognized. From a knowledge of the thermodynamic and kinetic behavior of these elements in the particular environment and in the alloys, it is possible to determine the suitability of the materials for high-temperature service. This approach has been used to analyze carburization-decarburization phenomena that involve austenitic stainless steels in sodium heat-transport systems of nuclear reactors.^{15,16} For this purpose, carbon activity-concentration relationships have been generated for Fe-Cr-8 wt pct Ni alloys with chromium contents between 0 and 22 wt pct in the temperature range of 725 to 1060°C. The experimental data, which were obtained at temperatures considerably lower than those reported in the literature, will be useful in establishing quantitative predictions of the carburization-decarburization behavior of austenitic stainless steels under different environmental conditions.

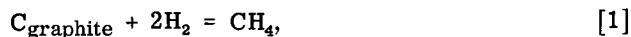
K. NATESAN and T. F. KASSNER are Metallurgists with the Materials Science Division, Argonne National Laboratory, Argonne, Ill. 60439.

Manuscript submitted March 6, 1973.

EXPERIMENTAL PROCEDURE

Apparatus

Measurements of carbon activity in the iron-base alloys were made by equilibrating foil samples in CH₄-H₂ gas mixtures of a fixed composition. The carbon activities in these materials as a function of temperature and carbon concentration were based upon two premises: first, the Elliott and Gleiser¹⁷ tabulation of the National Bureau of Standards (NBS)¹⁸ equilibrium data for the reaction



where the equilibrium constant ($K_{\text{eq}} = P_{\text{CH}_4} / P_{\text{H}_2}^2 a_C$) is represented by

$$\Delta G^\circ = -RT \ln (P_{\text{CH}_4} / P_{\text{H}_2}^2 a_C) = -21,550 + 26.16T \quad [2]$$

and secondly, carbon activities established from carbon concentrations in equilibrated nickel foils and the application of Henry's law to the solubility of carbon in nickel. The latter approach was included because it is known that the composition of CH₄-H₂ gas mixtures can be influenced by moisture contamination, and some difficulty could result in the determination of carbon activities in the materials solely from the gas composition. The desired carbon activities at each temperature were established by controlling the flow rate of ultrapure hydrogen and one of several mixed gases with 0.1, 1.0, and 5.0 pct methane in hydrogen, which corresponded to gas ratios calculated using Eq. [2]. The carbon concentrations in foil specimens of high-purity nickel were used to determine the actual carbon activities obtained in these experiments.

The equilibration experiments were conducted in a five-zone platinum-wound furnace that contained four 25 mm outside diam (OD) quartz reaction tubes. The samples were attached to a 5 mm OD thermocouple well provided in the center of the reaction tube that was closed at the bottom. The mixed gas entered through another 5 mm OD quartz tube attached to the inside of the reaction tube, passed through the sample

section, and exited at the top. The temperature in the vicinity of the samples was controlled within $\pm 1^\circ\text{C}$.

Carbon-activity measurements were also made by enclosing specimens of various iron-chromium-nickel alloys with a carbon source in evacuated quartz capsules and then annealing the capsules until carbon equilibrium was achieved in all specimens. The carbon activity attained within each capsule was determined from the final carbon content of the nickel and Fe-Ni alloys included in the capsules. In these experiments, the equilibrium carbon concentrations in the alloys were determined by specific CO/CO_2 ratios established by the carbon source.

Carbon-solubility values in nickel were also determined in the temperature range of 500 to 1000°C by equilibrating high-purity nickel foils with graphite rods in a flowing $\text{CH}_4\text{-H}_2$ gas mixture whose composition yielded a unit carbon activity. At temperatures between 800 and 1000°C , high-purity iron was included in these experiments; upon equilibration, the carbon concentrations were found to be in agreement with the reported graphite-solubility data, which indicated the validity of the experimental methods.

Materials and Analysis Procedure

The Fe-Cr-Ni alloys were arc melted from Armco iron, high-purity nickel and chromium in a 75 pct He-25 pct Ar atmosphere at a reduced pressure of 400 Torr. The castings were extruded, rolled and/or swaged to the desired thicknesses. All samples were solution annealed at 1025°C for 1 h prior to use in the carbon equilibration experiments. The compositions of the foil specimens of iron, nickel, and the iron-base alloys used in the carbon-activity measurements are given in Table I. Inasmuch as the temperature in the gas-phase equilibration experiments ranged between 500 and 1000°C , materials of several thicknesses were required to minimize the time for 99 pct equilibration, particularly at the lower temperatures. Materials of the following thicknesses were used: iron, 10 and 30 mils; nickel, 2, 5, and 12 mils; Fe-8 wt pct Ni, 2 and 10 mils; Fe-16 wt pct Ni, 2 mils; and Fe-Cr-8 wt pct Ni alloys, 1, 2, and 5 mils. The carbon-source samples, required for the capsule equilibration experiments, were obtained by carburizing iron, nickel, and

Table I. Composition of Iron, Nickel, and Iron-Base Alloys
(Concentrations are given in wt pct)

Alloy	Cr	Ni	C	N	O	Fe
Fe	<0.004	0.012	0.002	0.001	<0.007	Bal*†
Ni-270	<0.001	Bal*	0.002	0.001	<0.005	<0.01
Fe-8 wt pct Ni	<0.01	7.99	0.002	<0.001	0.016	Bal*
Fe-16 wt pct Ni	<0.001	15.87	0.003	<0.001	0.008	Bal*
Fe-8 wt pct Ni-2 wt pct Cr	1.96	7.92	0.002	<0.001	0.010	Bal*
Fe-8 wt pct Ni-4 wt pct Cr	3.89	7.86	0.004	<0.001	0.010	Bal*
Fe-8 wt pct Ni-8 wt pct Cr	7.90	7.90	0.004	<0.001	0.013	Bal*
Fe-8 wt pct Ni-12 wt pct Cr	11.96	7.96	0.003	<0.001	0.012	Bal*
Fe-8 wt pct Ni-15 wt pct Cr	14.74	7.82	0.003	<0.001	0.013	Bal*
Fe-8 wt pct Ni-18 wt pct Cr	17.74	7.92	0.003	0.002	0.008	Bal*
Fe-8 wt pct Ni-22 wt pct Cr	21.86	7.92	0.003	0.002	0.009	Bal*

*Bal indicates balance; spectrographic analyses for Mn, Mo, Si, Nb, Ti, Zr, V, Co, Cu indicated <0.01 wt pct.

†Manganese concentration in high-purity iron was 0.05 wt pct.

Fe-Ni alloys in CH_4/H_2 atmospheres between 800 and 1000°C .

The foil specimens were analyzed for carbon using a LECO low-carbon combustion analyzer that had a sensitivity of $\sim 5 \mu\text{g}$ of carbon for a 1-g sample. The analyzer was calibrated with a series of NBS iron-carbon alloy standards over the range of carbon values for the specimens in each run; a minimum of two analyses was made on each specimen. An examination of the Fe-Cr-Ni foils by optical and scanning electron microscopy ensured that the specimens were equilibrated in their entire cross section. The accuracy of carbon analyses was ± 2 pct for carbon concentrations above ~ 0.05 wt pct and ± 10 pct at carbon levels of ~ 0.005 wt pct in the materials.

EXPERIMENTAL RESULTS AND DISCUSSION

The results for the solubility of carbon in nickel at temperatures between 500 and 1000°C , shown in Fig. 1, are in good agreement with the higher temperature measurements of Wada *et al.*¹⁹ and Smith.²⁰ The combined data for the graphite solubility in nickel over the temperature range of 500 to 1200°C can be represented by the relation

$$C_{\text{Ni}} (\text{wt pct}) = 12.4 \exp(-5160/T). \quad [3]$$

The results of other investigators²¹⁻²⁵ were included in Fig. 1 for comparison. Wada *et al.* provided possible explanations for the somewhat larger carbon solubility values obtained in the other high-temperature investigations.²¹⁻²³

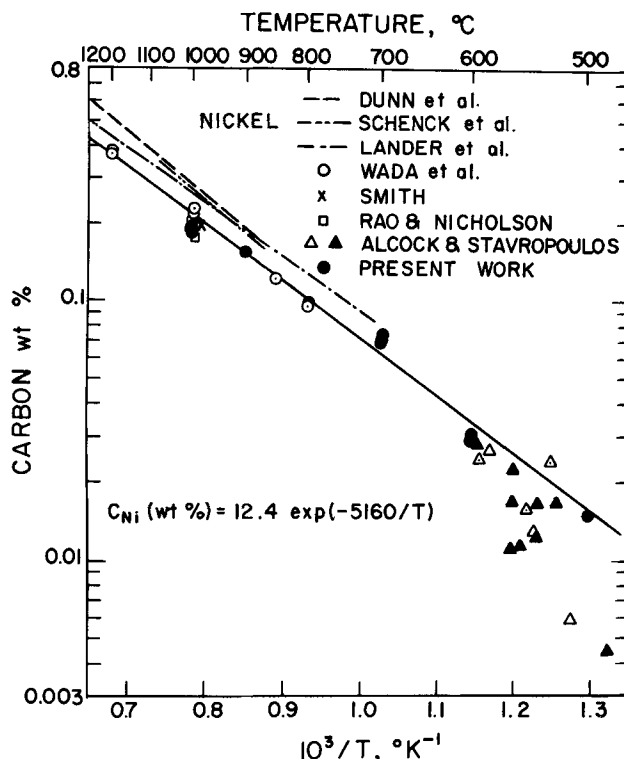


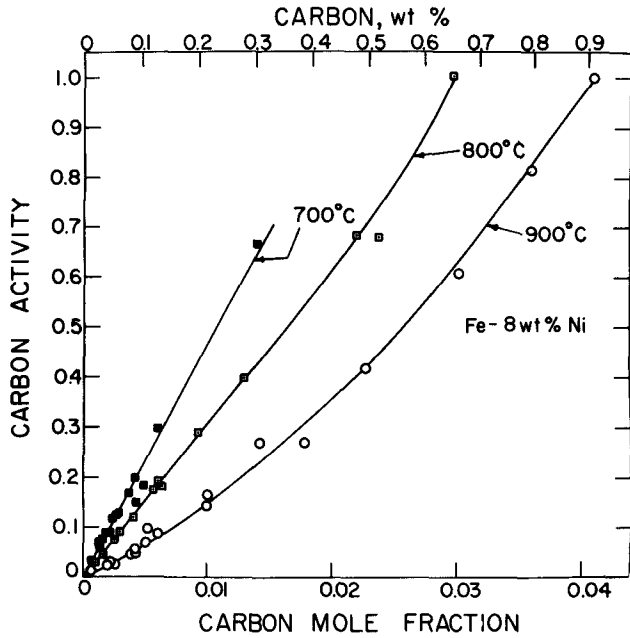
Fig. 1—Temperature dependence of the solubility of carbon in nickel.

Carbon Activity in Iron-Nickel Alloys

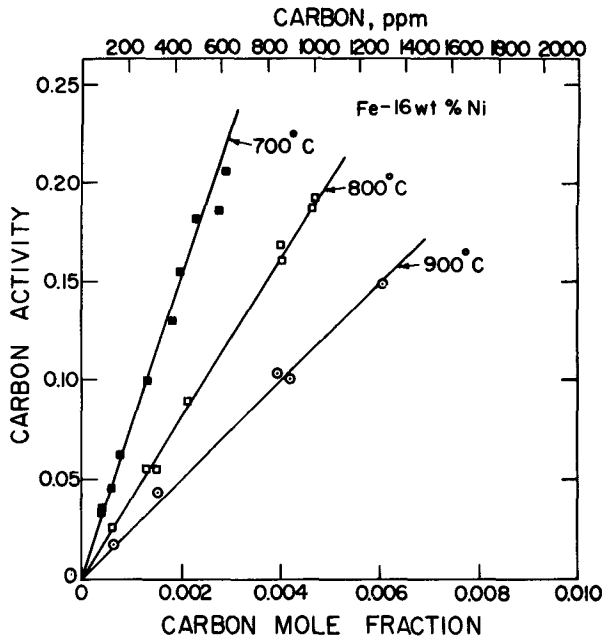
The carbon activity as a function of carbon concentration for Fe-8 wt pct Ni and Fe-16 wt pct Ni alloys was determined in the temperature range of 700 and 1060°C by equilibrating in CH₄-H₂ gas mixtures. The carbon activities* in the alloys were obtained from

*Carbon activities in this paper are based upon a graphite standard state.

carbon concentrations in nickel specimens that were included in the equilibration experiments and from application of Henry's law to the carbon solubility in nickel at various temperatures from Eq. [3]. The results are presented in Fig. 2 for the Fe-8 wt pct Ni and Fe-16 wt pct Ni alloys.



(a)



(b)

Fig. 2—Carbon activity-concentration relationship for the Fe-8 wt pct Ni and Fe-16 wt pct Ni alloys at 700, 800, and 900°C.

The effect of nickel on the activity of carbon in Fe-Ni-C alloys was determined from the data using a first-order free-energy interaction parameter to obtain a reliable extrapolation of the carbon-activity results to other temperatures and alloy compositions. The carbon activity ($a_C^{(FeNiC)}$) in the ternary system can be written as

$$a_C^{(FeNiC)} = \gamma_C^{(FeNiC)} N_C, \quad [4]$$

where

$$\gamma_C^{(FeNiC)} = \text{Raoultian activity coefficient for carbon in an Fe-Ni-C alloy,}$$

$$N_C = \text{mole fraction of carbon in an Fe-Ni-C alloy,}$$

and the activity coefficient $\gamma_C^{(FeNiC)}$ is given by

$$\ln \gamma_C^{(FeNiC)} = \ln \gamma_C^{(FeC)} + \epsilon_C^{Ni} N_{Ni}, \quad [5]$$

where

$$\gamma_C^{(FeC)} = \text{Raoultian activity coefficient for carbon in an Fe-C binary alloy,}$$

$$\epsilon_C^{Ni} = \text{free-energy interaction parameter for nickel on carbon}$$

$$= \left(\frac{\partial \ln \gamma_C}{\partial N_{Ni}} \right)_{N_{Fe} \rightarrow 1},$$

and

$$N_{Ni}, N_{Fe} = \text{mole fractions of nickel and iron in the alloy.}$$

Results of different investigators²⁶⁻³⁰ for the variation of the activity coefficient of carbon in austenite with carbon concentration in the Fe-C binary system are shown in Fig. 3. The curves at 700°C were extrapolated from the higher temperature data. Since there is no basis for selecting the results of a particular investigation, values of $\ln \gamma_C^{(FeC)}$ from the various stud-

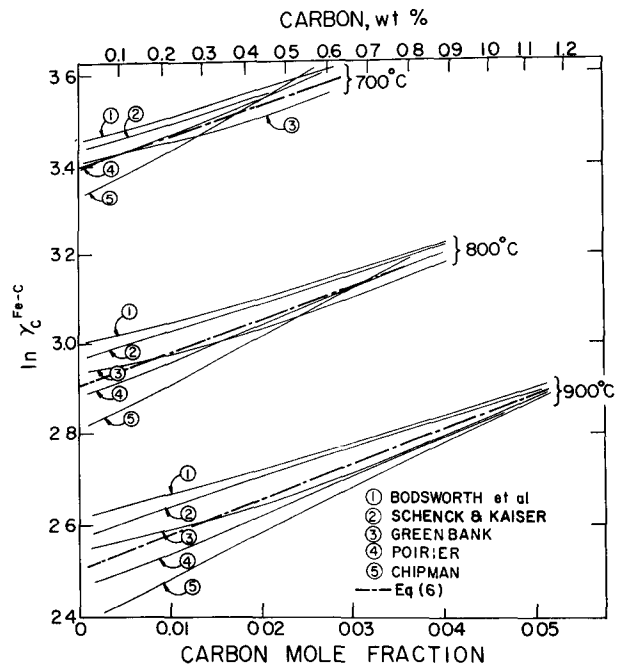


Fig. 3—The activity coefficient of carbon in Fe-C austenite as a function of carbon concentration obtained from the results of different investigators.²⁶⁻³⁰

ies were averaged to obtain the dashed curves in Fig. 3 which can be represented by the equation

$$\ln \gamma_C^{(\text{FeC})} = \ln \left(\frac{1}{1-N_C} \right) + \left(11.92 - \frac{6330}{T} \right) \left(\frac{N_C}{1-N_C} \right) - 1.845 + \frac{5100}{T} \quad [6]$$

The results of the different investigators are in good agreement; for example, the experimentally determined carbon activities are within ± 10 and ± 2 pct of the values computed using Eq. [6] for carbon mole fractions of 0.001 and 0.05, respectively, at 900°C. By combining Eqs. [5] and [6], a generalized mathematical relation can be obtained for the carbon-activity coefficient as a function of carbon concentration in iron-nickel-carbon alloys at various temperatures. The temperature dependence of interaction parameter ϵ_C^{Ni} , shown in Fig. 4, was obtained from a least-squares analysis of the results of this work and the data in the literature and can be represented by the relation

$$\epsilon_C^{\text{Ni}} = -2.2 + \frac{7600}{T} \quad [7]$$

Therefore, the carbon activity in the ternary Fe-Ni-C system becomes

$$\ln a_C^{(\text{FeNiC})} = \ln \left(\frac{N_C}{1-N_C} \right) + \left(11.92 - \frac{6330}{T} \right) \left(\frac{N_C}{1-N_C} \right) - 1.845 + \frac{5100}{T} - \left(2.2 - \frac{7600}{T} \right) N_{\text{Ni}} \quad [8]$$

The carbon-activity values calculated using Eq. [8] are compared, in Fig. 5, with the experimental data generated in the present work and those available in the literature^{19,20,28,31} for the temperature range of 700 to 1060°C.

Using the notation of Lupis and Elliott,^{32,33} the temperature dependence of ϵ_C^{Ni} can be written in terms of first-order enthalpy η_C^{Ni} , and entropy σ_C^{Ni} , coefficients

$$\epsilon_C^{\text{Ni}} = \frac{\eta_C^{\text{Ni}}}{RT} - \frac{\sigma_C^{\text{Ni}}}{R} \quad [9]$$

If η_C^{Ni} and σ_C^{Ni} are independent of temperature, a plot of ϵ_C^{Ni} vs $1/T$ should result in a straight line. As shown in Fig. 4, this is the case within experimental scatter of the results of the various investigations. Therefore, the enthalpy and entropy interaction parameters for the effect of nickel on carbon in Fe-Ni-C alloys are

$$\eta_C^{\text{Ni}} = 15,100 \text{ cal/mole (63,180 joules/mole)} \quad [10]$$

and

$$\sigma_C^{\text{Ni}} = 4.35 \text{ eu (18.2 joules/mole-K)} \quad [11]$$

Carbon Activity in Iron-Chromium-Nickel Alloys

The carbon activity-concentration relationships for the Fe-8 wt pct Ni and Fe-16 wt pct Ni alloys and the carbon-solubility values in nickel were used to establish carbon activities in Fe-Cr-8 wt pct Ni alloys whose chromium content ranged between 2 and 22 wt pct. The relation between the carbon and chromium concentrations in these alloys is shown in Figs. 6 and 7 by the isoactivity lines that were generated over a wide range

of carbon activities at temperatures between 725 and 1060°C. It is evident from these figures that the carbon concentration increases with an increase in chromium content of the Fe-Cr-8 wt pct Ni alloy for a given carbon activity and temperature. Furthermore, an increase in the chromium content of the alloy results in precipitation of carbide phases, particularly at lower temperatures and high carbon activities.

The influence of chromium on the carbon activity in these quaternary alloys can be evaluated by applying the interaction-parameter concept to the experimental data at low carbon activities and low chromium concentrations. The carbon activity in the Fe-Cr-8 wt pct Ni-C alloy, $a_C^{(\text{FeCr8NiC})}$, can be expressed as

$$a_C^{(\text{FeCr8NiC})} = \gamma_C^{(\text{FeCr8NiC})} N_C = \gamma_C^{(\text{Fe8NiC})} \gamma_C^{\text{Cr}} N_C, \quad [12]$$

where

$\gamma_C^{(\text{FeCr8NiC})}$ = Raoultian activity coefficient for carbon in the quaternary alloy;

$\gamma_C^{(\text{Fe8NiC})}$ = Raoultian activity coefficient for carbon in the Fe-8 wt pct Ni-C alloy and given by Eq. [6];

γ_C^{Cr} = Raoultian activity coefficient for carbon that results from chromium addition to the alloy;

and

N_C = mole fraction of carbon in the alloy.

Therefore, from Eq. [12]

$$\ln \gamma_C^{\text{Cr}} = \ln \left(\frac{\gamma_C^{(\text{FeCr8NiC})}}{\gamma_C^{(\text{Fe8NiC})}} \right), \quad [13]$$

where $\ln \gamma_C^{\text{Cr}}$ is a function of the mole fraction of chromium in the alloy.

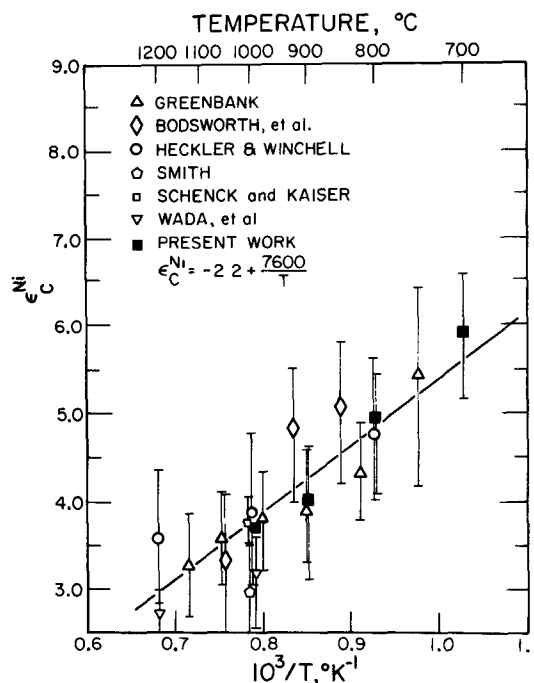


Fig. 4—Temperature dependence of the free-energy interaction parameter for nickel on carbon in Fe-Ni-C alloys.

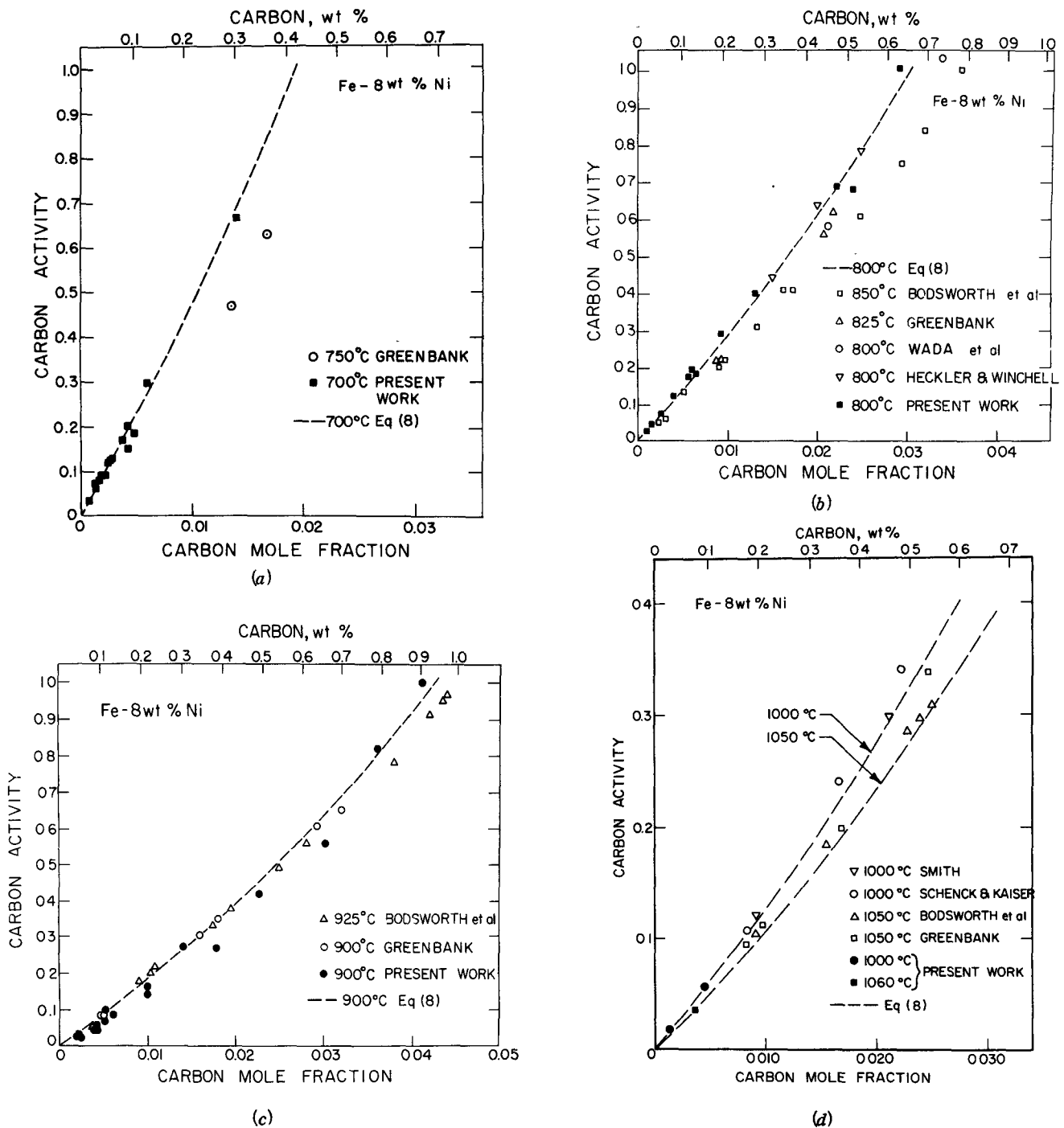


Fig. 5—Carbon activity-concentration relationship in Fe-8 wt pct Ni alloy at 700, 800, 900, 1000, and 1050°C.

The carbon-activity coefficient that results from the addition of chromium to the Fe-Ni-C alloy was evaluated as a function of the chromium mole fraction of the alloy from the experimental isoactivity lines presented in Figs. 6 and 7 at the various temperatures, and the results are given in Fig. 8. It should be noted that the values of $\ln \gamma_C^{Cr}$ at high chromium concentrations do not represent true activity coefficients for carbon because of the fact that the alloy is composed of a two-phase mixture of carbide and austenite. However, at low chromium concentrations (*i.e.*, 0 to 4 wt pct), the carbon-activity coefficient in the single-phase austen-

itic alloys can be related to the chromium mole fraction by

$$\ln \gamma_C^{Cr} = \left(\frac{\partial \ln \gamma_C}{\partial N_{Cr}} \right)_{N_{Fe} \rightarrow 1} N_{Cr} = \epsilon_C^{Cr} N_{Cr}, \quad [14]$$

where

ϵ_C^{Cr} = free-energy interaction parameter for chromium on carbon, and

N_{Cr} = mole fraction of chromium in the alloy.

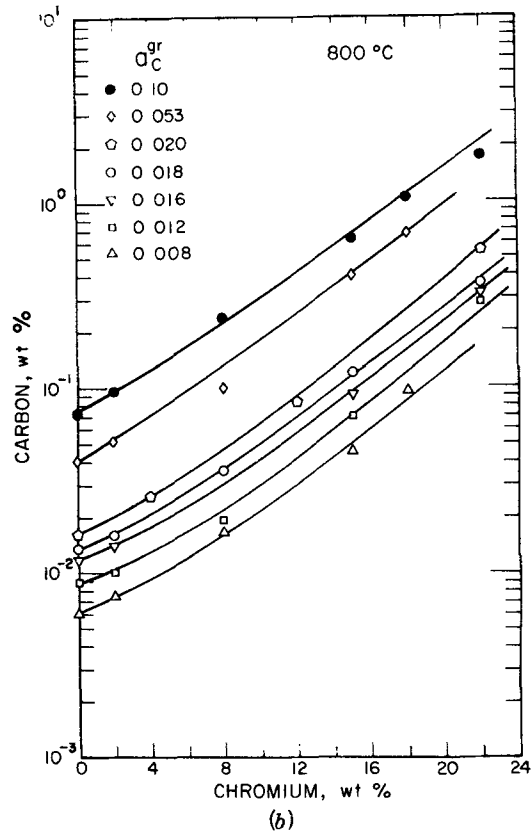
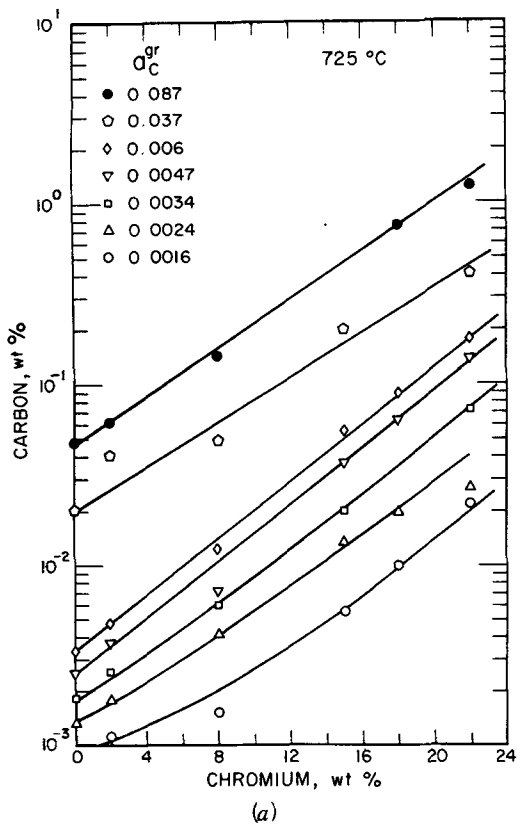


Fig. 6—Isoactivity lines for carbon in Fe-Cr-8 wt pct Ni alloys at 725 and 800°C.

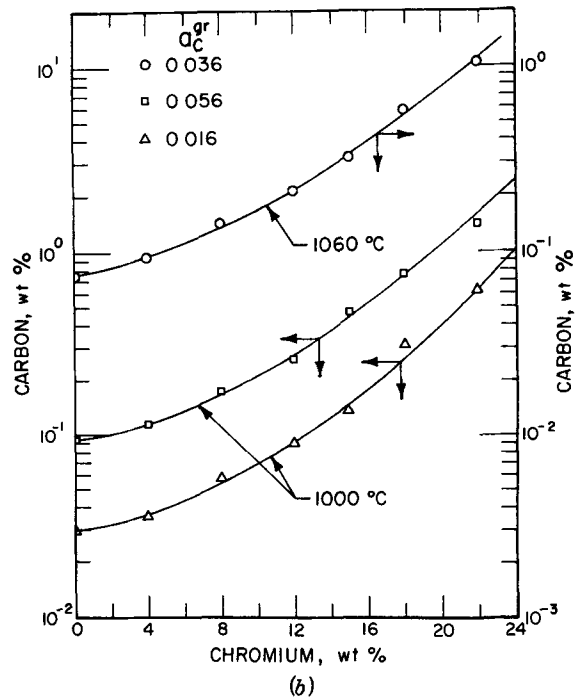
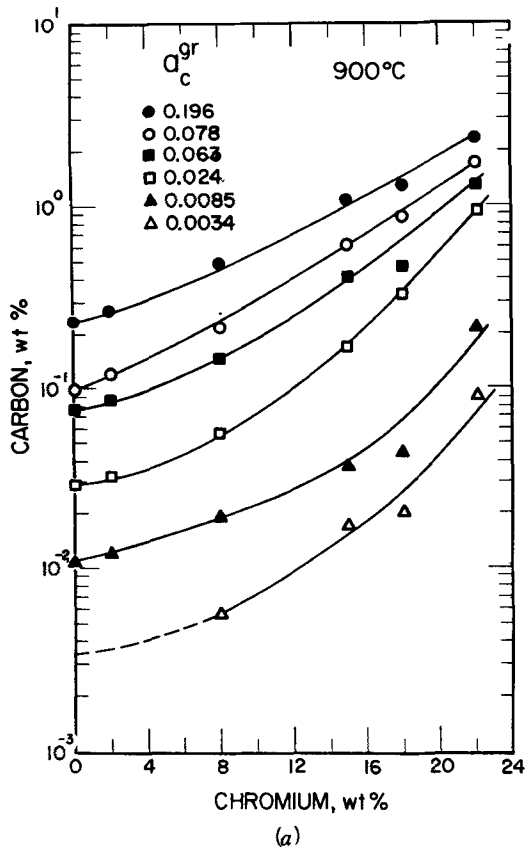


Fig. 7—Isoactivity lines for carbon in Fe-Cr-8 wt pct Ni alloys at 900, 1000, and 1060°C.

Fig. 9 shows the interaction parameter ϵ_C^{Cr} as a function of temperature obtained from the present work, which can be represented by the expression

$$\epsilon_C^{Cr} = 24.4 - \frac{38,400}{T} \quad [15]$$

As before, the temperature dependence of ϵ_C^{Cr} can be written in terms of first-order enthalpy η_C^{Cr} and en-

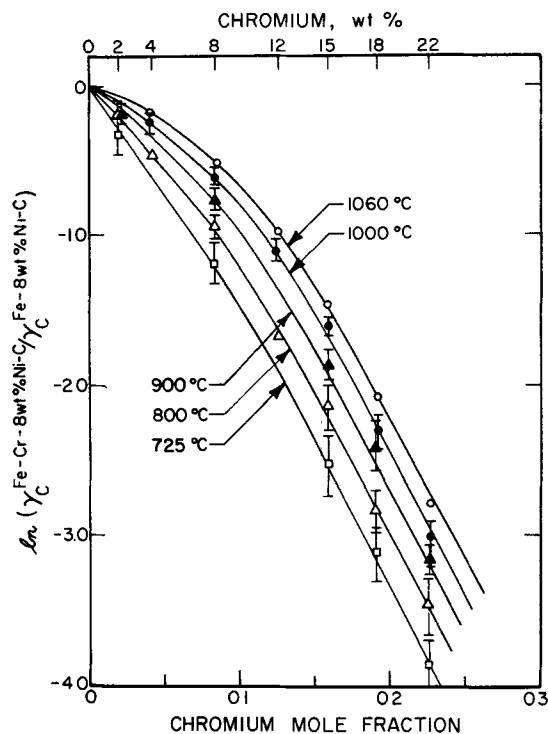


Fig. 8—The effect of chromium on the activity coefficient of carbon in Fe-Cr-8 wt pct Ni-C alloys at various temperatures.

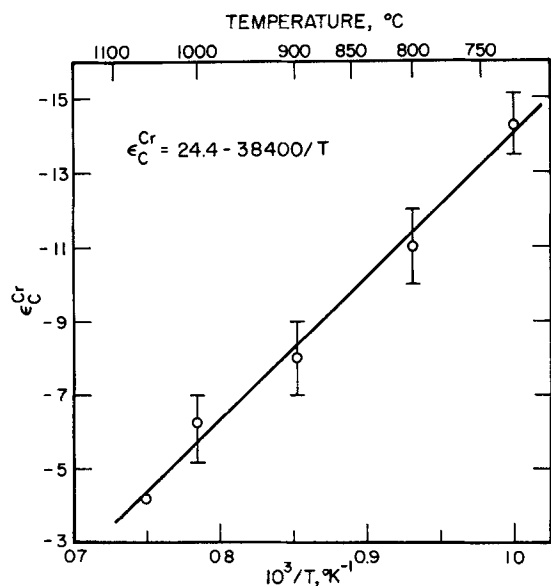


Fig. 9—Temperature dependence of the free-energy interaction parameter for chromium on carbon in Fe-Cr-8 wt pct Ni-C alloys with low chromium concentrations.

tropy σ_C^{Cr} , coefficients whose values are

$$\eta_C^{Cr} = -76,300 \text{ cal/mole } (-319,240 \text{ joules/mole}) \quad [16]$$

and

$$\sigma_C^{Cr} = -48.5 \text{ eu } (-202.9 \text{ joules/mole-K}) \quad [17]$$

In addition to evaluating the thermodynamic interaction parameters for carbon from the experimental data at low carbon activities and low chromium contents in the alloys, it is also desirable to obtain an expression that relates the carbon activities to the carbon and chromium concentrations over the entire range of

chromium contents (0 to 22 wt pct) and temperatures (725 to 1060°C) investigated in this work. For this purpose, γ_C^{Cr} in Eq. [14] was expressed as

$$\ln \gamma_C^{Cr} = \epsilon_C^{Cr} N_{Cr} + \rho_C^{Cr} N_{Cr}^2, \quad [18]$$

and ρ_C^{Cr} was evaluated as a function of temperature to represent the data in Fig. 9. It should be noted that ρ_C^{Cr} in Eq. [18] has no direct thermodynamic significance, since the alloy at the high chromium levels is composed of a two-phase (carbide + austenite) mixture. The value of ρ_C^{Cr} evaluated at various temperatures is plotted in Fig. 10 and can be expressed by the relation

$$\rho_C^{Cr} = -96.8 + \frac{84,800}{T}. \quad [19]$$

Therefore, the carbon activity in the quaternary Fe-Cr-Ni-C system in the composition range of 0 to 16 wt pct Ni and 0 to 22 wt pct Cr becomes

$$\begin{aligned} \ln a_C^{(FeCrNiC)} = & \ln \left(\frac{N_C}{1-N_C} \right) + \left(11.92 - \frac{6330}{T} \right) \left(\frac{N_C}{1-N_C} \right) \\ & - 1.845 + \frac{5100}{T} - \left(2.2 - \frac{7600}{T} \right) N_{Ni} \\ & + \left(24.4 - \frac{38,400}{T} \right) N_{Cr} \\ & - \left(96.8 - \frac{84,800}{T} \right) N_{Cr}^2 \quad [20] \end{aligned}$$

The carbon-activity values calculated using Eq. [20] are compared, in Fig. 11, with the experimental data generated in the present work (Figs. 6 and 7) at temperatures of 725, 800, 900, and 1000°C. It is evident from these figures that there is good agreement between the carbon-activity values calculated from Eq. [20] and the experimental data points.

For comparison of these results with data in the literature, it is useful to relate the carbon activity to the alloy composition in weight percent units given by Eq. [21].

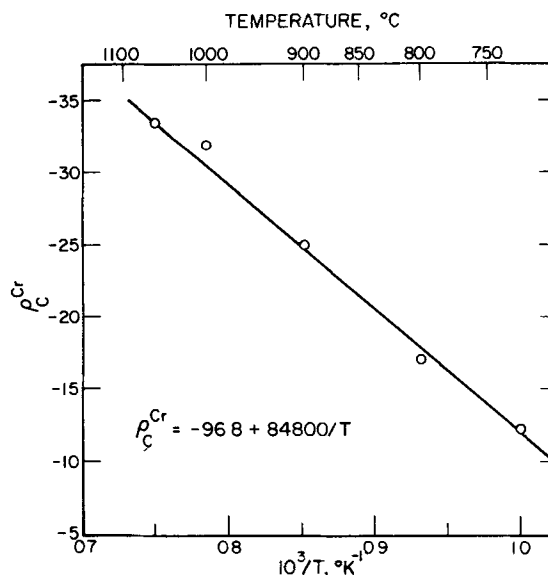


Fig. 10—Temperature dependence of the second-order coefficient in Eq. [18] that is used to describe the effect of chromium on the carbon-activity coefficient in Fe-Cr-8 wt pct Ni-C alloys with chromium contents up to 22 wt pct.

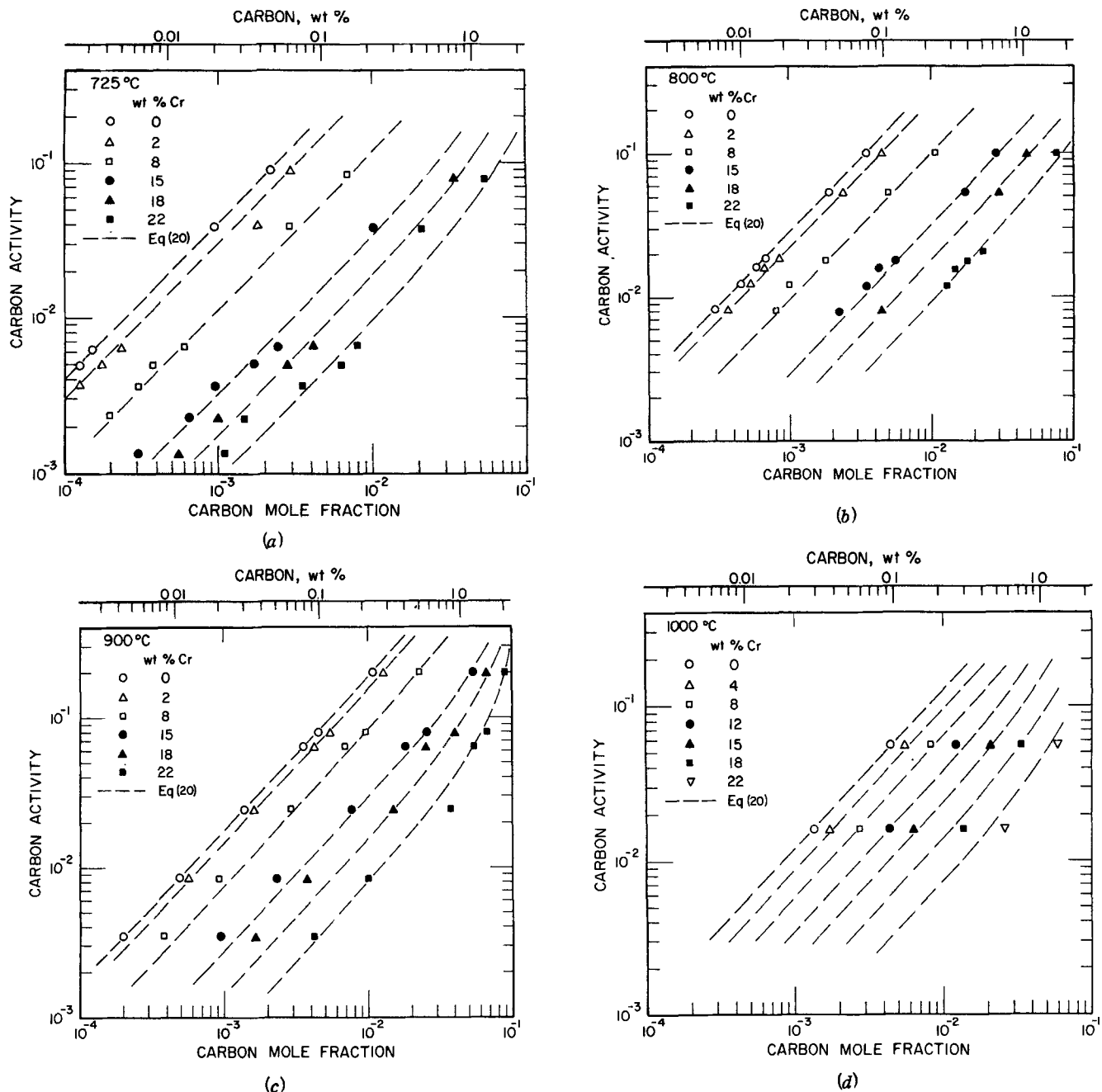


Fig. 11—The carbon activity-concentration relationship in Fe-Cr-8 wt pct Ni-C alloys at 725, 800, 900, and 1000°C. The dashed lines in this figure were calculated using Eq. [20].

$$\ln a_{\text{C}}^{(\text{FeCrNiC})} = \ln (0.048 \text{ pct C}) + \left(0.525 - \frac{300}{T}\right) \text{ pct C} - 1.845 + \frac{5100}{T} - \left(0.021 - \frac{72.4}{T}\right) \text{ pct Ni} + \left(0.248 - \frac{404}{T}\right) \text{ pct Cr} - \left(0.0102 - \frac{9.422}{T}\right) \text{ pct Cr}^2. \quad [21]$$

Carbon-activity data obtained by a number of investigators^{28,30,34-38} for Fe-Cr-C alloys with chromium contents between 3.35 and 5.00 wt pct at 1000 to 1050°C are replotted in Fig. 12 after converting their carbon activities to a common Fe-C baseline (*i.e.*, the first four terms in Eqs. [20] and [21]) that was used in this work.

The carbon activity-concentration relationships calculated using Eq. [20] for an Fe-4 wt pct Cr alloy at 1000 and 1050°C, indicated by the dashed lines in this figure, are in good agreement with the results of Bodsworth *et al.*,³⁰ Brigham and Kirkaldy,³⁴ Wada *et al.*,³⁷ and Greenbank.³⁸

Greenbank³⁹ equilibrated a number of Fe-Cr-Ni alloys with iron in methane-hydrogen gas mixtures at temperatures between 900 and 1050°C. The chromium and nickel content of the alloys and the carbon concentrations after equilibration are given in Tables II and III as well as the carbon content of the iron that was included in each run. The carbon activities obtained from the carbon concentrations in iron and the Fe-Cr-Ni alloys using Eq. [21] are in excellent agreement for

Table II. Comparison of Carbon Activities from Eq. [21] Based Upon the Carbon Concentrations in Iron and Fe-Cr-Ni Alloys of Different Composition Equilibrated at 900°C from the Work of Greenbank³⁹

Composition of Equilibrated Fe-Cr-Ni-C Alloys			Carbon Concentration in Iron, Pct C	Carbon Activity	
Pct Cr	Pct Ni	Pct C		a_{C}^{Fe}	$a_{\text{C}}^{\text{(FeCrNi)}}$
4.10	0.60	0.200	0.138	0.084	0.082
3.12	1.62	0.177	0.138	0.084	0.084
2.22	2.54	0.158	0.138	0.084	0.086
1.41	3.61	0.135	0.138	0.084	0.083
0.53	4.52	0.117	0.138	0.084	0.081
4.10	0.60	0.607	0.422	0.277	0.279
3.12	1.62	0.543	0.422	0.277	0.285
2.22	2.54	0.483	0.422	0.277	0.286
1.41	3.61	0.431	0.422	0.277	0.286
0.53	4.52	0.382	0.422	0.277	0.283
4.10	0.60	2.24	1.070	0.837	1.60
3.12	1.62	1.745	1.070	0.837	1.27
2.22	2.54	1.345	1.070	0.837	1.14
1.41	3.61	1.097	1.070	0.837	0.870
0.53	4.52	0.979	1.070	0.837	0.852
8.52	1.04	0.105	0.038	0.023	0.025
6.04	3.09	0.070	0.038	0.023	0.025
4.67	4.88	0.052	0.038	0.023	0.023
2.70	7.03	0.038	0.038	0.023	0.023
1.00	8.61	0.024	0.038	0.023	0.018
8.52	1.04	0.364	0.122	0.074	0.092
6.04	3.09	0.213	0.122	0.074	0.077
4.67	4.88	0.173	0.122	0.074	0.079
2.70	7.03	0.127	0.122	0.074	0.078
1.00	8.61	0.098	0.122	0.074	0.076
8.52	1.04	1.090	0.420	0.276	0.336
6.04	3.09	0.680	0.420	0.276	0.280
4.67	4.88	0.549	0.420	0.276	0.277
2.70	7.03	0.427	0.420	0.276	0.284
1.00	8.61	0.342	0.420	0.276	0.283

Table III. Comparison of Carbon Activities from Eq. [21] Based Upon the Carbon Concentrations in Iron and Fe-Cr-Ni Alloys of Different Composition Equilibrated at 1050°C from the Work of Greenbank³⁹

Composition of Equilibrated Fe-Cr-Ni-C Alloys			Carbon Concentration in Iron, Pct C	Carbon Activity	
Pct Cr	Pct Ni	Pct C		a_{C}^{Fe}	$a_{\text{C}}^{\text{(FeCrNi)}}$
4.10	0.60	0.116	0.082	0.030	0.033
3.12	1.62	0.103	0.082	0.030	0.033
2.22	2.54	0.091	0.082	0.030	0.032
1.41	3.61	0.080	0.082	0.030	0.030
0.53	4.52	0.071	0.082	0.030	0.029
4.10	0.60	0.308	0.230	0.088	0.092
3.12	1.62	0.278	0.230	0.088	0.093
2.22	2.54	0.260	0.230	0.088	0.095
1.41	3.61	0.229	0.230	0.088	0.091
0.53	4.52	0.211	0.230	0.088	0.091
4.10	0.60	0.602	0.460	0.189	0.198
3.12	1.62	0.546	0.460	0.189	0.197
2.22	2.54	0.493	0.460	0.189	0.193
1.41	3.61	0.450	0.460	0.189	0.191
0.53	4.52	0.411	0.460	0.189	0.188
4.10	0.60	1.380	1.092	0.542	0.571
3.12	1.62	1.275	1.092	0.542	0.572
2.22	2.54	1.195	1.092	0.542	0.577
1.41	3.61	1.098	1.092	0.542	0.565
0.53	4.52	1.020	1.092	0.542	0.559
8.52	1.04	0.122	0.066	0.024	0.023
6.04	3.09	0.109	0.066	0.024	0.028
4.67	4.88	0.086	0.066	0.024	0.027
2.70	7.03	0.061	0.066	0.024	0.024
1.00	8.61	0.050	0.066	0.024	0.023
8.52	1.04	0.450	0.223	0.085	0.094
6.04	3.09	0.346	0.223	0.085	0.096
4.67	4.88	0.290	0.223	0.085	0.096
2.70	7.03	0.230	0.223	0.085	0.094
1.00	8.61	0.191	0.223	0.085	0.091
8.52	1.04	0.790	0.419	0.170	0.182
6.04	3.09	0.606	0.419	0.170	0.182
4.67	4.88	0.511	0.419	0.170	0.179
2.70	7.03	0.415	0.419	0.170	0.178
1.00	8.61	0.347	0.419	0.170	0.173
8.52	1.04	1.150	0.509	0.212	0.295
6.04	3.09	0.725	0.509	0.212	0.226
4.67	4.88	0.625	0.509	0.212	0.227
2.70	7.03	0.510	0.509	0.212	0.225
1.00	8.61	0.420	0.509	0.212	0.214
14.65	15.53	0.130	0.062	0.023	0.019
14.65	15.53	0.375	0.109	0.040	0.056
14.65	15.53	0.400	0.131	0.049	0.060
14.65	15.33	0.960	0.203	0.077	0.172

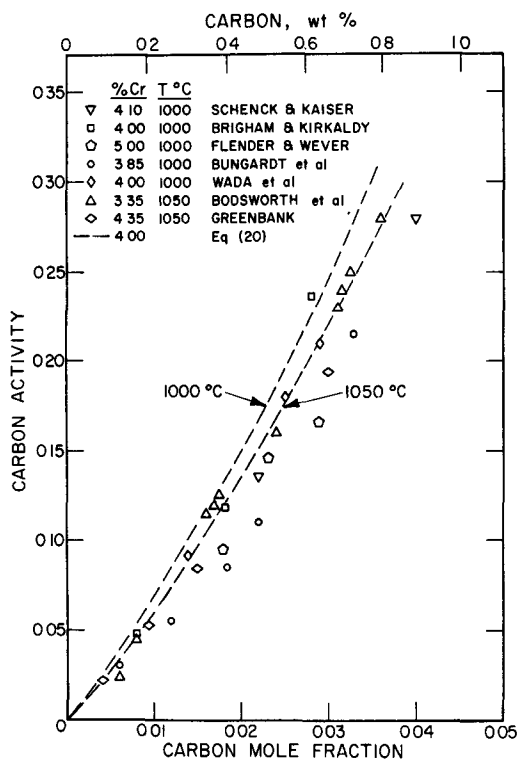


Fig. 12—Comparison of carbon-activity results from this work with data in the literature^{29,30,34-38} for Fe-Cr alloys with 3.35 to 5.0 wt pct Cr at 1000 and 1050°C.

carbon concentrations in the alloys below ~1.0 wt pct. These results further indicate that the interaction effect of chromium and nickel on the carbon activity in Fe-Cr-Ni alloys and its variation with temperature have been adequately expressed by Eqs. [20] and [21] for chromium and nickel concentrations in the range of 0 to 22 and 0 to 16 wt pct, respectively.

ACKNOWLEDGMENTS

The Jones and Laughlin Steel Corporation and the Armco Steel Corporation supplied some of the alloys used in this work. The Materials Science Division Fabrication Technology Group cast some of the alloys and produced the foil specimens. D. L. Rink assisted with the experimental program. This work was performed under the auspices of the U. S. Atomic Energy Commission.

REFERENCES

1. K. J. Irvine, T. Gladman, and F. B. Pickering: *J. Iron Steel Inst.*, 1969, vol. 207, p. 1017.
2. J. E. White and J. W. Freeman: *Trans. ASME, J. Eng. Power*, 1963, vol. 85, p. 119.
3. R. Nakagawa and Y. Ootoguro: *Tetsu-To-Hagane*, 1961, vol. 47, p. 1169.
4. Y. Kawabe, R. Nakagawa, and T. Mukoyama: *Trans. Iron Steel Inst. Jap.*, 1968, vol. 8, no. 6, p. 353.
5. L. M. T. Hopkin and L. H. Taylor: *J. Iron Steel Inst.*, 1967, vol. 205, p. 17.
6. P. D. Goodell, T. M. Cullen and J. W. Freeman: *Trans. ASME, J. Basic Eng.*, 1967, vol. 89, p. 517.
7. P. G. Stone: *High Temperature Properties of Steels*, p. 505, Proc. Joint Conf. organized by BISRA and ISI, 1966.
8. I. A. Rohrig: *Effects of Residual Elements on Properties of Austenitic Stainless Steels*, p. 78, ASTM-STP 418, 1966.
9. J. K. Y. Hum and N. J. Grant: *Trans. ASM*, 1953, vol. 45, p. 105.
10. J. T. Barnby and F. M. Peace: *Acta Met.*, 1971, vol. 19, p. 1351.
11. R. Stickler and A. Vinckier: *Trans. ASM*, 1961, vol. 54, p. 362.
12. H. F. Ebling and M. A. Scheil: *Advances in the Technology of Stainless Steels and Related Alloys*, p. 275, ASTM-STP 369, 1965.
13. B. Weiss and R. Stickler: *Met. Trans.*, 1972, vol. 3, p. 851.
14. G. F. Tisinai, J. K. Stanley, and C. H. Samans: *Trans. AIME*, 1954, vol. 200, p. 1259.
15. K. Natesan and T. F. Kassner: *J. Nucl. Mater.*, 1970, vol. 37, p. 223.
16. K. Natesan and T. F. Kassner: *Proc. of Symposium on Chemical Aspects of Corrosion and Mass Transfer in Liquid Sodium*, S. A. Jansson, ed., p. 130, AIME, 1972.
17. J. F. Elliott and M. Gleiser: *Thermochemistry for Steelmaking*, Addison-Wesley Publishing Company, Cambridge, Mass., 1960.
18. *Selected Values of Chemical Thermodynamic Properties*, National Bureau of Standards, Ser. III, 1948.
19. T. Wada, H. Wada, J. F. Elliott, and J. Chipman: *Met. Trans.*, 1971, vol. 2, p. 2199.
20. R. P. Smith: *Trans. TMS-AIME*, 1960, vol. 218, p. 62.
21. W. W. Dunn, R. B. McLellan, and W. A. Oates: *Trans. TMS-AIME*, 1968, vol. 242, p. 2129.
22. H. Schenck, M. G. Froberg, and E. Jaspert: *Arch. Eisenhüttenw.*, 1965, vol. 36, p. 683.
23. J. J. Lander, H. E. Kern, and A. L. Beach: *J. Appl. Phys.*, 1952, vol. 23, p. 1305.
24. K. K. Rao and M. E. Nicholson: *Trans. TMS-AIME*, 1963, vol. 227, p. 1029.
25. C. B. Alcock and G. P. Stavropoulos: *Trans. Inst. Mining Met.*, Section C, 1968, vol. 77, p. 232.
26. J. Chipman: *Trans. TMS-AIME*, 1967, vol. 239, p. 2.
27. D. R. Poirier: *Trans. TMS-AIME*, 1968, vol. 242, p. 685.
28. J. C. Greenbank: *J. Iron Steel Inst.*, 1971, vol. 209, p. 819.
29. H. Schenck and H. Kaiser: *Arch. Eisenhüttenw.*, 1960, vol. 31, p. 227.
30. C. Bodsworth, I. M. Davidson, and D. Atkinson: *Trans. TMS-AIME*, 1968, vol. 242, p. 1135.
31. A. J. Heckler and P. G. Winchell: *Trans. TMS-AIME*, 1963, vol. 227, p. 732.
32. C. H. P. Lupis and J. F. Elliott: *Trans. TMS-AIME*, 1965, vol. 233, p. 820.
33. C. H. P. Lupis and J. F. Elliott: *Acta Met.*, 1966, vol. 14, p. 529.
34. R. J. Brigham and J. S. Kirkaldy: *Trans. TMS-AIME*, 1963, vol. 227, p. 538.
35. H. Flender and H. Wever: *Arch. Eisenhüttenw.*, 1963, vol. 34, p. 727.
36. K. Bungardt, H. Preisendanz, and G. Lehnert: *Arch. Eisenhüttenw.*, 1964, vol. 35, p. 999.
37. T. Wada, H. Wada, J. F. Elliott, and J. Chipman: *Met. Trans.*, 1972, vol. 3, p. 2865.
38. J. C. Greenbank: *J. Iron Steel Inst.*, 1971, vol. 209, p. 986.
39. J. C. Greenbank: *J. Iron Steel Inst.*, 1972, vol. 210, p. 111.